Fast, whole-cell DNA-PAINT imaging with dual-labeled self-quenched imager probes

Arindam Ghosh[#*], Mara Meub[#], Dominic A. Helmerich, Sören Doose, and Markus Sauer[*]

Department of Biotechnology and Biophysics, Biocenter, University of Würzburg, Am Hubland, 97074 Würzburg, Germany

#These authors contributed equally

*Corresponding authors (A.G. arindam-ghosh@uni-wuerzburg.de; M.S. m.sauer@uni-wuerzburg.de)

Abstract

In DNA-PAINT, background fluorescence emerging from unbound imager probes requires the use of low imager concentrations, reducing the imaging speed substantially. Here, we present a novel class of dual-labeled probes that show strong fluorescence quenching when unbound, enabling imaging at higher probe concentrations with an up to ~15-fold increase in imaging speed and improved resolution. We demonstrate two-dye imager DNA-PAINT (TDI-DNA-PAINT) imaging in cells and on DNA origami. Finally, we demonstrate lattice light-sheet (LLS)-TDI-DNA-PAINT for fast whole-cell three-dimensional (3D) imaging with superior spatial resolution.

Introduction

DNA-based points accumulation for imaging in nanoscale topography (DNA-PAINT) relies on transient binding of a fluorophore-tagged single-stranded short oligonucleotide probe (imager strand) to a complementary oligonucleotide (docking strand) attached at the target of interest[1]. Several key benefits of DNA-PAINT include the possibility to achieve sub-10 nm spatial resolution using a conventional widefield/TIRF microscope[2], easy multiplexing via sequential imaging of targets of interest with different imager strands (exchange-PAINT)[3], and resilience to photobleaching of fluorophores as they are constantly replenished by freely diffusing imager strands in solution. Nevertheless, a major issue remains to be the background signal originating from freely diffusing imager probes in solution. As such, classical DNA-PAINT applications have been realized using probe concentrations of 0.1-0.5 nM, thereby resulting in long durations of data acquisition, typically in the range of a few hours. Lately, efforts have been made to engineer smarter fluorogenic imager probes in order to improve DNA-PAINT imaging. In particular, two main classes of fluorogenic probes have been reported: a) probes end-labeled with a dye and a quencher molecule so that the fluorescence signal of the emitter is efficiently quenched via energy transfer[4] or dye-quencher contact in the unbound state[5] to enable faster imaging at higher probe concentrations and b) probes end-labeled with two identical dyes which form non-fluorescent dimers in the unbound state[6,7]. The non-fluorescent dimer strategy has been used very recently to demonstrate stimulated emission depletion and super-resolution localization microscopy with increased spatial resolution[7].

In order to exploit non-fluorescent dimer formation for faster DNA-PAINT imaging, we tested different dyes to improve the dimer formation efficiency and identified ATTO Oxa14 (earlier known as MR121) as a superior-performing dye for the synthesis of self-quenched DNA and peptide probes that efficiently forms non-fluorescent H-dimers (Fig. S1)[6,8]. The underlying concept involves the formation of quenched imager probes that show minimal fluorescence in the unbound state whereas the fluorescence signal will be completely revived upon transient binding to the complementary docking strand (Fig. 1a). We term this modality as two-dye imager DNA-PAINT or TDI-DNA-PAINT.

Results and Discussion

For the first demonstration of TDI-DNA-PAINT, we selected a routinely used classical DNA-PAINT imager strand P3 (10 nucleotides)[1] and the speed optimized R4 (7 nt)[2] and labeled them with one or two ATTO Oxa14 dyes. In the remainder of the manuscript, we will refer to the dual-labeled and single-labeled imagers as Ox2-(P3 or R4) and Ox1-(P3 or R4), respectively. Ensemble fluorescence emission spectra of Ox2-P3 in the absence and presence of a 10^4-molar excess of docking strand showed an 8.7-fold increase in fluorescence intensity in the bound state (Fig. 1b). Ox2-R4 probes displayed a similar fluorescence quenching efficiency (Fig. S2a). Furthermore, we confirmed the formation of non-fluorescent H-dimers between the two terminal ATTO Oxa14 dyes by fluorescence correlation spectroscopy (FCS). Here, we assumed that the conformational flexibility of the imager strand permits contact formation of the two dyes. The halving of the FCS amplitude upon addition of an excess of

docking strands demonstrates that on average ~ 50% of all dual-labeled probes form non-fluorescent H-dimers with a lifetime that is longer than the diffusion time through the confocal detection volume (~1 ms) (Fig. 1c). In addition, shorter-lived dimer formation (indicated by the correlation decay on µs time scales) and collisional quenching reduces the fluorescence of undocked imager strands.

Following spectroscopic investigations, we utilized Ox2 probes for imaging microtubules in COS7 cells. Efficient fluorescence quenching of ATTO Oxa14 dual-labeled probes in the unbound state allowed us to use Ox2-P3 and Ox2-R4 at substantially higher concentrations (Fig. S2b). Therefore, we could use Ox2-P3 at a concentration of 5 nM, whereas classical DNA-PAINT with Ox1-P3 had to be conducted at 100 pM concentrations. Five minutes of imaging resulted in 31,400, 27,100, and 2,490 detected localizations for the two TDI-DNA-PAINT imager strands Ox2-R4 and Ox2-P3, and the classical DNA-PAINT imager strand Ox1-P3, respectively, for an image area covered with comparable filament density (Fig. 1d). For classical DNA-PAINT, the mean localization precision from three independent 60 min measurements with Ox1-P3 was found to be 5.3 nm. In contrast, after 10 min of TDI-DNA-PAINT imaging, we obtained localization precisions of 4.4 nm and 4.1 nm for Ox2-P3 and Ox2-R4 imagers, respectively (Fig. 1e)[9]. This corresponds to an improvement factor of 1.20 and 1.29 for Ox2-P3 and Ox2-R4 probes, respectively. The higher localization precision results from the higher signal-to-noise (SNR) of dual-labeled imager probes in the bound, unquenched state and the higher fluorescence intensity in the bound state due to the presence of two fluorophores (Fig. 1f and Fig. S2c). Interestingly, the attachment of two fluorophores per imager strand has only little influence on the binding time (on-time) demonstrating that TDI-DNA-PAINT can be easily implemented using established imager sequences (Fig. S2d). For a more precise estimation of the imaging speed, we computed the number of localizations (blinks) detected for TDI-DNA-PAINT and DNA-PAINT per micrometer of filament and per unit time (Fig. 1g). In case of DNA-PAINT (Ox1-P3), we detected 0.2 ± 0.02 blinks $\mu m^{-1}s^{-1}$, whereas for TDI-DNA PAINT at 50-fold higher imager concentration we detected 2.6 ± 0.06 and 2.9 ± 0.04 blinks $\mu m^{-1}s^{-1}$ for Ox2-P3 and Ox2-R4 probes, respectively, resulting in a 13-fold and 14.5-fold increase in effective imaging speed (Fig. 1g).

Next, we utilized the speed-optimized Ox2-R4 probe for imaging a DNA origami with four docking strands separated by 18 nm (Fig. 1h)[10]. The defined two-dimensional DNA origami sample with 4 docking sites allowed us to use higher TDI-DNA-PAINT imager concentrations of up to 25 nM. Already after 5 minutes imaging with Ox2-R4 at a concentration of 25 nM, we detected 24-35 localizations per DNA origami and could successfully resolve the 18 nm inter-fluorophore distance (Fig. 1i and Fig. S2e-f). On average, we detected an inter-fluorophore distance of 18.9 ± 2.2 nm (SEM) at an acquisition time of 5 minutes (Fig. 1j).

The intuitive inference from our 2D TDI-DNA-PAINT imaging results is that self-quenched Ox2 probes should be extremely beneficial for fast volumetric imaging, especially with excitation schemes such as selective-plane illumination (SPIM)[11-13]. To this end, we realized TDI-DNA-PAINT using lattice light sheet microscopy (LLS) for whole-cell imaging of microtubule networks (Fig. 2a). LLS relies on selective-plane illumination of samples with a light-sheet of sub-micron to micron thickness for volumetric imaging at isotropic resolution in 3D (Fig. 2b). LLS-based three-dimensional (3D) astigmatic PALM[12], *d*STORM[13],

and PAINT with fluorogenic probes[14] has been implemented previously using the original upright microscope design. Here, spatial resolutions of up to ~60-70 nm in lateral and ~100-110 nm in axial direction have been achieved but required long acquisition times of up to several days for densely labeled whole cells[14]. Since TDI-DNA-PAINT provides higher spatial resolutions, lower background, and higher SNR (Fig. 1f and Fig. S2b), and a substantial reduction in acquisition time, we concluded that it represents the ideal method for whole-cell super-resolution fluorescence imaging with superior spatial resolution.

For realization of fast, whole-cell 3D TDI-DNA-PAINT we used a commercially available inverted LLS microscope equipped with high-power lasers. Using a light-sheet thickness of 1.8 µm and a new astigmatism approach[15] enabled us to perform 3D TDI-DNA-PAINT of whole COS7 cells immunolabeled for microtubules (Fig. 2a-c and Fig. S3a-c). We acquired 2,500 frames per position along the skewed *y* axis and a total of 35 positions with an interval of 0.5 µm (~0.25 µm along true *z* of the coverslip coordinates). Using a TDI-DNA-PAINT imager probe concentration of 2.5 nM, we detected 21.3 million localizations for Ox2-R4 and 17.5 million localizations for Ox2-P3 within a 4 hour acquisition time from an acquired volume of 87 µm × 72 µm × 8.8 µm. Reconstructed images of COS7 cells imaged with Ox2-R4 (Fig. 2a) and Ox2-P3 (Fig. S3a) imager probes demonstrate the practical feasibility of fast, volumetric LLS-TDI-DNA-PAINT. We achieved localization precisions in the range of 24 ± 12 nm and 59 ± 22 nm (s.d.) along the *x* and *z* axis, respectively, for Ox2-P3 and slightly higher precisions of 14 ± 5 nm and 53 ± 15 nm along the *x* and *z* axis, respectively, for Ox2-R4 (Fig. 2d). The slightly higher localization precision of Ox2-R4 is likely due to gliding of the imager probe along the docking strand caused by the presence of repetitive binding sequences. The achieved overall localization precisions are comparable to previous reports but are substantially lower than those achieved in our 2D experiments due to the lower numerical aperture (NA) of 1.0 of our commercial inverted LLS microscope. Furthermore, as already observed in previous LLS-PAINT experiments, individual microtubule filaments far away from the coverslip can be visualized at high spatial resolutions but the localization precision was worse in the central region of cells due to higher emitter densities (Fig. 2c)[14]. In addition, we had to reduce the imager probe concentration from 5 nM for 2D to 2.5 nM for 3D imaging to accommodate for the width of astigmatic patterns.

Recently, we demonstrated that energy transfer interactions between fluorophores separated by less than 10 nm prevent reliable molecular resolution fluorescence imaging with photoswitchable fluorophores independent of the localization precision of the method[9]. Hence, to realize the full potential of sub-nanometer localization precision methods such as MINFLUX[16] or MINSTED[17], they have to use DNA-PAINT or photoactivatable fluorophores ensuring that two adjacent fluorophores are never present or photoactivated simultaneously. Since in DNA-PAINT, the achievable localization precision does not only scale with the number of detected photons per localization but also with the number of localizations acquired per target it can likewise achieve superior resolution[2]. Unfortunately, such high spatial resolutions come along with extremely long acquisition times impeding large field of view nanometer resolution imaging.

Most recently, self-quenched imager probes labeled with two ATTO 655 dyes were used to demonstrate STED microscopy and DNA-PAINT with reduced background contribution from unbound imager strands at slightly higher photon budget[7]. However, here by using an oxazine dye with superior H-dimer formation tendency[6,8] we could successfully tackle the main problem of DNA-PAINT imaging, which is long acquisition times. The substantially reduced fluorescence background of ATTO Oxa14 labeled self-quenched imager probes enables the use of higher imager probe concentrations and consequently up to 15-fold higher imaging speed with higher localization precision as compared to classical DNA-PAINT. The reduced background fluorescence and increased imaging speed provides the basis for whole-cell 3D LLS-TDI-DNA-PAINT imaging within a few hours. Since TDI-DNA-PAINT works with established DNA-PAINT sequences it can be easily adopted and does not require the design of optimized docking and imager strands as necessary for FRET-based approaches[4,5]. Thus, TDI-DNA-PAINT can also be advantageously used to speed up multiplexed DNA-PAINT imaging approaches[18]. Among the screened fluorophores, TDI-DNA-PAINT with ATTO Oxa14 outperformed Cy5, ATTO 655, and tetramethlyrhodamine (Fig. S4). However, a careful screening for other fluorophores with stronger H-dimer formation efficiency might pave the way for even more efficient and faster LLS-TDI-DNA-PAINT at true molecular resolution[2].

Methods

Imager and docking DNA strands. Methyltetrazine modified docking strands P3': MetTet-5′-TTTCTTCATTA-3′ and 7xR4': MetTet- 5'-ACACACACACACACACACA-3'; imager probes P3: 5'-GTAATGAAGA-3' singly and double labeled with the dyes Cy5, ATTO655, TMR, and ATTO Oxa14 (Ox2-P3). R4: 5'-TGTGTGT-3' double labeled with ATTO Oxa14 (Ox2-R4) were obtained commercially from biomers.net GmbH.

Imaging buffers. Imaging buffer for microtubules in COS7 cells: PBS (Sigma-Aldrich, D8537-500 ML) + 500 mM NaCl (Sigma-Aldrich, S5886) at pH 7.4**.** Imaging buffer for DNA-Origami samples: PBS (Sigma-Aldrich, D8537-500 ML) + 5 mM TRIS (Invitrogen, AM9855G) + 50 mM $MgCl_2$ (AppliChem, A4425,0500) + 1 mM EDTA (Sigma, E1644-250G) + 0.05% Tween20 (ThermoFisher, 28320) adjusted to pH 7.6.

Cell culture. African green monkey kidney fibroblast-like cells (COS7, Cell Lines Service GmbH, Eppelheim, #605470) were cultured in DMEM (Sigma, #D8062) containing 10% FCS (Sigma-Aldrich, #F7524), 100 U/mL penicillin and 0.1 mg/mL streptomycin (Sigma-Aldrich, #P4333) at 37 °C and 5% CO_2. Cells were grown in standard T25-culture flasks (Greiner Bio-One).

Antibody modification for TDI-DNA-PAINT imaging of microtubules. For labeling of goat anti-rabbit IgG (H+L) secondary antibody (Invitrogen, 31212) with PEG4-TCO, an excess of TCO-PEG4-NHS was used. Antibody labeling was performed at 20°C for 4 hours in labeling buffer (100 mM sodium tetraborate (Fulka, 71999), pH 9.5) following the manufacturer's standard protocol. Goat anti-rabbit IgG (H+L) secondary antibody was reconstituted in labeling buffer using 0.5 mL spin-desalting columns (40K MWCO, ThermoFisher, 87766). The conjugated antibody was purified using spin-desalting columns and

stored in PBS. Finally, the antibody concentration was determined by UV–vis absorption spectrometry (Jasco V-650).

Immunostaining of microtubules. COS7 cells were seeded at concentrations of 2.5 × 10^4 cells/well into eight-well chambered glass slides with a high-performance cover glass bottom (Cellvis, C8-1.5H-N). Cells were grown until proper adhesion at 37°C and 5% CO_2. Cells were washed with pre-warmed (37°C) PBS and permeabilized for 2 minutes using 0.3% glutaraldehyde (GA) + 0.25% Triton X-100 (EMS, 16220 and ThermoFisher, 28314) in pre-warmed (37 °C) cytoskeleton buffer (CB) which consists of 10 mM MES ((Sigma-Aldrich, M8250), pH 6.1), 150 mM NaCl, 5 mM EGTA (Sigma-Aldrich, 03777), 5 mM glucose (Sigma-Aldrich, G7021), and 5 mM $MgCl_2$ (AppliChem, A4425,0500). Following permeabilization, cells were fixed with a pre-warmed (37 °C) solution of 2% GA for 10 min. After GA-induced fixation, cells were incubated for 5 minutes in 100 mM glycine (Ajinomoto, G5417) to stop fixation followed by washing twice with PBS. Samples were reduced with 0.1% sodium borohydride (Sigma-Aldrich, 71320) in PBS for 7 minutes to avoid background fluorescence, and again washed three times with PBS. After blocking with 5% BSA (Roth, #3737.3) for 30 minutes, cells were incubated with primary antibody (rabbit anti-alpha tubulin antibody, Abcam, ab18251, 5 µg/ml) for 1 hour at 20°C followed by three washing steps with PBS. Next, cells were incubated with secondary goat anti-rabbit IgG labeled with PEG4-TCO (10 µg/mL) for 1 hour at 20 °C and again washed three times with PBS. After washing, cells were incubated with MetTet-5′-TTTCTTCATTA-3′ or MetTet- 5'-ACACACACACACACACACA-3' single-stranded docking DNA strands (biomers.net GmbH, custom-made, 10 µg/mL) for 15 minutes at RT. The methyltetrazine modification allowed the attachment of docking strands to secondary antibody via 'click chemistry'. As a last step, cells were washed three more times with PBS (Sigma-Aldrich, D8537-500 ML) and stored at 4 °C until imaging.

DNA origami surface preparation. DNA-origami single-molecule surfaces were prepared in eight-well chambers (following the exact described protocol[9]) containing high performance cover glass (Cellvis, C8-1.5H-N). The wells were washed once with PBS (Sigma-Aldrich, D8537-500ML) before treatment with 2% Hellmanex (Hellma, 9-307-011-4-507) for 1 hour. Following the treatment, the chambers were washed three times with PBS. Next, the surfaces were incubated with 1 M KOH (Fulka, 06005) for 20 minutes followed and washed three times with PBS. Next, the surfaces were incubated with 10% polyethylene glycol 400 (Fulka, 81170) overnight at 4 °C. On the following day, the surfaces were rinsed thrice with PBS and the chambers were incubated with 0.5 g/l BSA-Biotin (ThermoFisher, 29130) in PBS overnight at 4 °C. Next day, the chambers were washed again thrice with PBS before incubation with 0.5 g/l Neutravidin (ThermoFisher, 31050) in PBS for 20 minutes. The surfaces were washed three times with PBS and incubated with purified DNA-origami solution, 1:5 diluted in PBS + 50 mM $MgCl_2$ (AppliChem, A4425,0500) for 10 minutes. The prepared samples were washed at least thrice with PBS + 50 mM $MgCl_2$ before imaging.

Preparation of DNA-origami structures. Design, hybridization and quality control of DNA-origami rectangular structures were carried out as described earlier in Helmerich et al.[9], using the same DNA sequences and the final 18 nm spaced structure. Briefly, sequences were designed with caDNAno v.2.2.0 and stability calculations of the origami designed were performed using CanDO [18-20]. We obtained the trans-cyclooctene (TCO) modified staple strands from biomers.net GmbH, biotinylated

strands from Sigma-Aldrich, and unmodified staple strands from Merck KGaA. The scaffold DNA used in this study was phage M13mp18 derivate DNA type p7560 (tilibit nanosystems, M1-32). We performed the hybridization reaction by mixing 10 nM scaffold DNA with 15× surplus of unmodified staple strands and 30× surplus of modified staple strands in hybridization buffer (5 mM tris(hydroxymethyl)aminomethane (TRIS) (Merck, 1.08382.2500), 5 mM sodium chloride (NaCl) (Sigma, S5880-1KG), 1 mM ethylene diamine tetra-acetic acid (EDTA) (Sigma, E1644-250G) and 12 mM magnesium chloride ($MgCl_2$) (AppliChem, A4425,0500)) using a ThermoCycler (C1000 Thermal Cycler, BioRad) by applying a linear thermal gradient of −1 °C min^{-1} from 90 to 4 °C. In case of origami samples for TDI-DNA-PAINT, TCO modified staple strands were used. After hybridization, the origami nanostructures were incubated with a 10× surplus of docking strands (P3': MetTet-5′-TTTCTTCATTA-3′ or 7xR4': MetTet- 5'-ACACACACACACACACACA-3') per TCO-staple for overnight at 4°C. Finally, the clicked and hybridized samples were purified by gel electrophoresis using a 1.5% agarose gel (Sigma, A9539-500G) in 1× TBE buffer, consisting of 4.5 mM TRIS, 4.5 mM boric acid, 10 mM EDTA. A 0.5× TBE was used as running buffer. A final concentration of 12 mM $MgCl_2$ was added to all TBE buffers.Finally, extracted agarose gel parts were divided by cutting several times and purified via Freeze N′ Squeeze columns (Freeze N′ Squeeze, 7326165, BioRad) according to the manufacturer's instructions using a benchtop centrifuge (Biofuge fresco, Heraeus) at 13,000*g*. For all measurements, the DNA origami were produced freshly and imaged immediately.

Ensemble absorbance and fluorescence spectroscopy. UV / visible absorbance spectra and steady-state fluorescence emission spectra of fluorescently labeled imager probes were recorded using a Jasco V650 absorbance spectrometer and Jasco FP-6500 spectrofluorometer respectively. For absorbance spectra, 500 nM Ox2 and Ox1 imagers were used (Supplementary Fig. S1). In case of fluorescence spectra, 1 nM imager strands and respective docking strands were used in 10^4 molar excess (10 µM). Supplementary Fig. S2 shows fluorescence emission spectra of 2×ATTO655, 2×Cy5, and 2×TMR imager strands. Samples were measured in a 3 mm path-length cuvette (Hellma, 105.251-QS) in PBS (Sigma-Aldrich, D8537-500ML) containing 500 mM NaCl adjusted at pH 7.4.

Fluorescence correlation spectroscopy (FCS). FCS measurements on Ox2-P3 probes (Figure 1c) were carried out using a commercial time-resolved confocal fluorescence microscope setup (MicroTime200, PicoQuant) as described previously [21]. Imager strands were used at a concentration of 1 nM dissolved in PBS (Sigma-Aldrich, D8537-500ML) containing 500 mM NaCl adjusted at pH 7.4, while the complementary docking strand was 10^4 times higher i.e., 10 µM.

TDI-DNA-PAINT imaging. TDI-DNA-PAINT imaging of microtubules in COS7 cells was done utilizing an inverted wide-field fluorescence microscope (IX-71; Olympus). For excitation of Ox2 probes, a 640 nm diode laser (Cube 640-100C, Coherent) in combination with a clean-up filter (laser clean-up filter 640/10, Chroma) was used. The laser beam was focused onto the back focal plane of the oil-immersion objective (100×, NA 1.51; Olympus). Emission light was separated from the illumination light using a dichroic mirror (HC 560/659; Semrock) and spectrally filtered by a band-pass filter (FF01-679/41-25, Semrock). Images were recorded with an electron-multiplying CCD camera chip (iXon DU-897; Andor). Pixel size for data analysis was measured to be 104 nm. For classical DNA-PAINT and TDI-DNA-PAINT experiments, 5 nM Ox2-P3 / Ox2-R4 probe and 100 pM Ox1-P3 probe was added to respective glass-

bottomed chamber wells containing COS7 cells fixed and immunolabeled with corresponding MetTet-P3' docking strand (Figure 1d). Blinking movies (Supplementary Movies S1-S12,) were recorded for representative 128 × 128-pixel areas with TIRF excitation with an exposure time of 150 ms (frame rate 6.6 Hz) and irradiation intensity of 0.8 kW/cm^2. Images were recorded for 24k frames (one hour) for each dataset. We recorded images of DNA-origami samples using a different setup but with same optical parameters and components as for the previous one. We used this second setup as it is a more robust "drift-free" system in our laboratory and can be beneficial for origami samples. We added 25 nM of Ox2-R4 probes to the well containing DNA-origami nanostructures labeled with MetTet -7×R4' docking strand incubated in the imaging buffer for origami. Images were recorded for 128 × 128-pixel areas (Movie S3) with exposure times of 30 ms for 90k frames at 1.1 kW/cm^2. Pixel size for data analysis was measured to be 128 nm.

Data analysis. TDI-DNA-PAINT data for microtubules and DNA-origami were analyzed using the MATLAB-based Super-resolution Microscopy Analysis Platform (SMAP)[22]. Using SMAP, data analysis was done by following the steps: loading of camera images, filtering, background estimation, finding of candidate molecules, fitting, and saving of the results. First, we loaded the raw blinking movies into the SMAP GUI, which was followed by manually setting up the camera parameters. Next, under the *Localize\Peak Finder* tab, we set the parameters for the initial estimation of single molecule positions, such as filtering cutoff with intensity values. To ensure selecting the brightest localizations, we select a higher cutoff value, such as in Extended data Fig. 1c preview frame. After previewing an exemplary frame, we chose the Gaussian 2D fitting tab *PSF free* for localizing the full image set. The analysis returns coordinates such as x, y and z, number of photons per localization, background values, localization precisions, frame in which localization was found etc. Grouping (merging) of localizations persistent over several frames is performed after fitting. We can manually set the following grouping parameters dX (maximum distance two localizations can be apart) and dT (maximum number of dark frames between localizations). We grouped the localizations by setting dT = 1, and limiting the localization precision range from 0-15 nm, which filters out localizations with worse precision. On applying these grouping parameters, SMAP calculates the maximum distance from the localization precision of the two candidate localizations. That means that localizations are only grouped if it is likely they stem from the same event. We also quantified the background signal from different concentrations of Ox2-P3/R4 probes from 100 pM to 10 nM, and 5 nM appeared to be the most optimal concentration considering it had very similar background as compared to 100 pM Ox1-P3 (Extended data Fig. 1b). We also tested if the attachment of two fluorophores to the imager P3 introduced any change to binding time (on-time). Extended data Fig.1 d-f depict the on-time comparison between Ox1-P3,Ox2-P3, and Ox2-R4 which were found to be 1.76, 1.97, and 1.47 frames respectively. Extended data Fig. 1g-j presents photon yields, localization precision, background signal, and detected origami structures from TDI-DNA-PAINT experiments with Ox2-R4. The reported distances from origami experiments were from N = 33 values.

Data availability

The data that support the findings of this study will be provided by the corresponding author upon reasonable request.

Acknowledgements

The authors thank Lukas Kapitein, Ralf Jungmann, and Mike Heilemann for fruitful discussions. A.G., D.A.H. and M.S. received funding from the European Research Council (ERC) under the European Union's Horizon 2020 research and innovation programme (grant agreement No 835102).

Author contributions

A.G. and M.S. conceived the project and wrote the manuscript. A.G. performed 2D TDI-DNA-PAINT and LLS-TDI-DNA-PAINT imaging of microtubules, analyzed the data, and generated the figures in main manuscript. M.M. did cell culture, prepared microtubule samples, did experiments on DNA origami, and helped in manuscript editing. D.A.H synthesized DNA origami platforms, prepared the final sample, and helped in manuscript editing. S.D. helped in data analysis and manuscript editing.

Competing interests

The authors declare no conflict of interest.

References

1. Schnitzbauer, J. et al. Super-resolution microscopy with DNA-PAINT. *Nat. Protoc.* **12.6**, 1198-1228 (2017).
2. Reinhardt, S. C. et al. Ångström-resolution fluorescence microscopy. *Nature* **617.7962**, 711-716 (2023).
3. Jungmann, R. et al. Multiplexed 3D cellular super-resolution imaging with DNA-PAINT and Exchange-PAINT. *Nat. Methods* **11.3**, 313-318 (2014).
4. Auer, A. Fast, background-free DNA-PAINT imaging using FRET-based probes. *Nano Lett.* **17.10**, 6428-6434 (2017).
5. Chung, K. K. et al. Fluorogenic DNA-PAINT for faster, low-background super-resolution imaging. *Nat. Methods* **19.5**, 554-559 (2022).
6. Knemeyer, J. P. et al. Self-quenching DNA probes based on dye dimerization for identification of mycobacteria. *Int. J. Environ. Anal. Chem.* **85**, 625-637 (2005).
7. Kessler, L. F. et al. Self-quenched Fluorophore Dimers for DNA-PAINT and STED Microscopy. *Angew. Chem. Int. Ed. Engl.* e202307538 (2023).
8. Bollmann, S. et al. Dimer formation of organic fluorophores reports on biomolecular dynamics under denaturing conditions. *Phys. Chem. Chem. Phys.* **13.28**, 12874-12882 (2011).
9. Mortensen, K. I., Churchman, L. S., Spudich, J. A., & Flyvbjerg, H. Optimized localization analysis for single-molecule tracking and super-resolution microscopy. *Nat. Methods*, **7.5**, 377-381 (2010).
10. Helmerich, D. A. et al. Photoswitching fingerprint analysis bypasses the 10-nm resolution barrier. *Nat. Methods* **19.8**, 986-994 (2022).
11. Huisken, J. et al. Optical sectioning deep inside live embryos by selective plane illumination microscopy. *Science* **305.5686**, 1007-1009 (2004).

12. Chen, B. C. et al. Lattice light-sheet microscopy: imaging molecules to embryos at high spatiotemporal resolution. *Science* **346.6208**, 1257998 (2014).
13. Wäldchen, F. et al. Whole-cell imaging of plasma membrane receptors by 3D lattice light-sheet *d*STORM. *Nat. Commun.* **11**, 887 (2020).
14. Legant, W. R. et al. High-density three-dimensional localization microscopy across large volumes. *Nat. Methods* **13.4**, 359-365 (2016).
15. Iwanski, M. K., Katrukha, E. A., & Kapitein, L. C. Lattice light-sheet motor-PAINT: a method to map the orientations of microtubules in complex three-dimensional arrays. *Single Molecule Analysis, Methods mol. biol.* https://link.springer.com/book/9781071633762.
16. Balzarotti, F. et al. Nanometer resolution imaging and tracking of fluorescent molecules with minimal photon fluxes. *Science* **355**, 606–612 (2017).
17. Weber, M., von der Emde, H., Leutenegger, M. *et al.* MINSTED nanoscopy enters the Ångström localization range. *Nat Biotechnol.* **41**, 569–576 (2023).
18. Unterauer, E. M. et al. Spatial proteomics in neurons at single-protein resolution. bioRxiv preprint doi: https://doi.org/10.1101/2023.05.17.541210.
19. Liedl, T., Högberg, B., Tytell, J., Ingber, D. E., & Shih, W. M. Self-assembly of three-dimensional prestressed tensegrity structures from DNA. *Nat. Nanotechnol.***5**, 520-524 (2010).
20. Kim, D. N., Kilchherr, F., Dietz, H., & Bathe, M. Quantitative prediction of 3D solution shape and flexibility of nucleic acid nanostructures. *Nucleic Acids Res.* **40**, 2862-2868 (2012).
21. Castro, C. et al. A primer to scaffolded DNA origami. *Nat. Methods* **8**, 221-229 (2011).
22. Ghosh, A., & Enderlein, J. Advanced fluorescence correlation spectroscopy for studying biomolecular conformation. *Curr. Opin. Struct. Biol.* **70**, 123-131 (2021).
23. Ries, J. SMAP: a modular super-resolution microscopy analysis platform for SMLM data. *Nat. Methods*, **17**, 870-872 (2020).

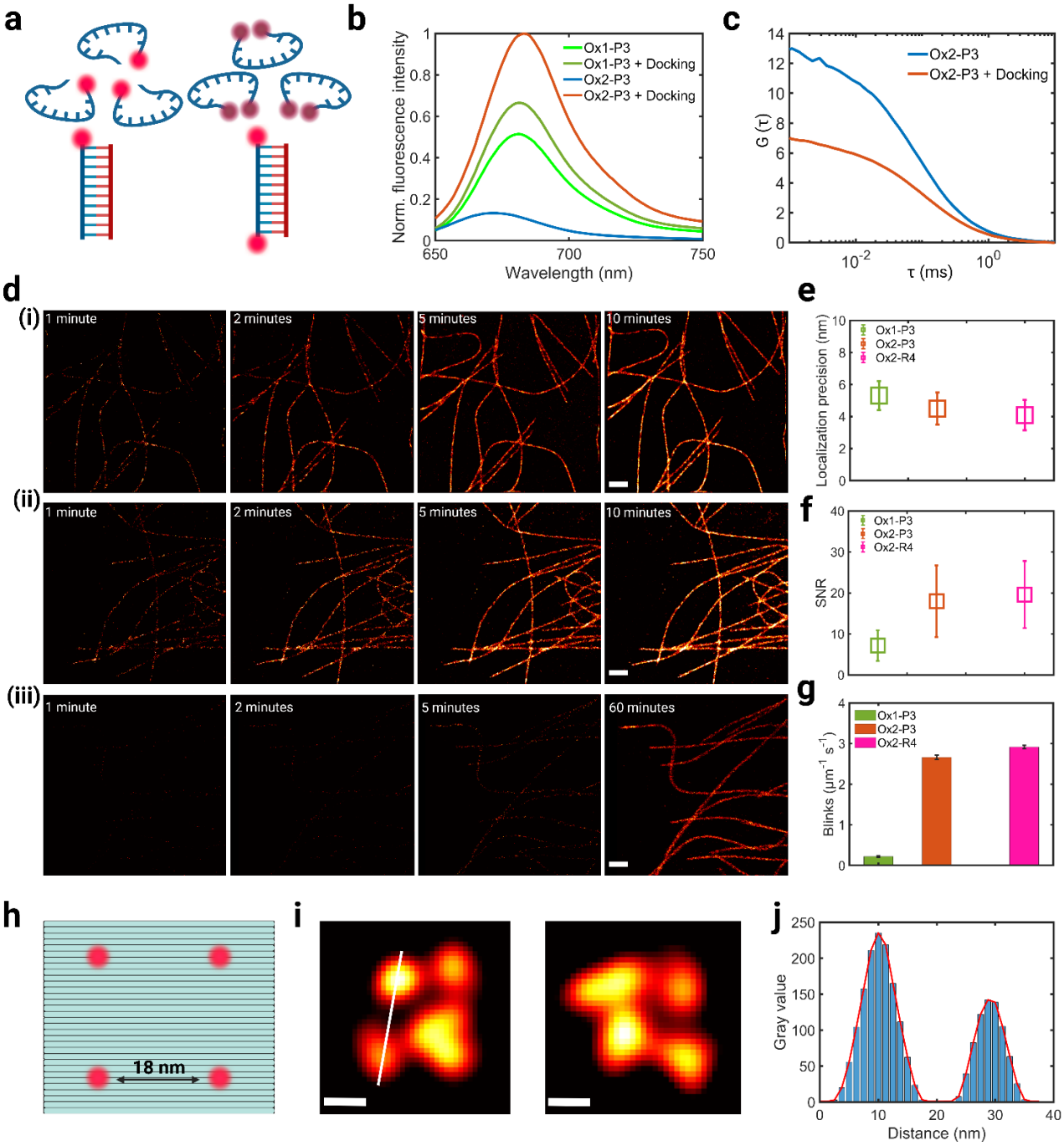

Fig. 1. TDI-DNA-PAINT imaging. a, Classical DNA-PAINT with single-labeled imagers (left) and TDI-DNA-PAINT workflow with dual-labeled Ox2 imagers (right). **b**, Fluorescence spectra of Ox1-P3 and Ox2-P3 in unbound state (neon green and blue respectively) and fluorescence dequenching after adding an excess of docking strands (green and red respectively). **c**, FCS measurement of Ox2-P3 before (blue) and after addition (red) of docking strand. **d**, TDI-DNA-PAINT imaging of microtubules with (i) 5 nM of Ox2-P3 probe. Reconstructions shown for 1, 2, 5, and 10 min. of data acquisition (upper row). (ii) 5 nM of Ox2-R4 probe. Reconstructions shown for 1, 2, 5, and 10 min. of data acquisition (middle row). (iii) Classical DNA-PAINT with 100 pM of Ox1-P3. Reconstructions shown for 1, 2, 5, and 60 minutes of image acquisition (lower row). Scale bars, 1 μm. **e**, Localization precisions (nm) after 5 min of TDI-DNA-PAINT imaging (Ox2-P3: red and Ox2-R4: magenta) were 4.5 ± 1.0 and 4.1 ± 0.9 nm respectively, whereas classical DNA-PAINT (Ox1-P3: green) experiment yielded a precision of 5.3 ± 0.9 nm after 60 minutes of data acquisition. **f**, Signal-to-noise ratio (SNR) comparison from experiments shown in **d.** We obtained mean SNR of 7.2, 18, and 19.6 for Ox1-P3, Ox2-P3 and -R4 probes respectively. **g,** Number of blinking events per μm per second for Ox1-P3 (green), Ox2-P3 (red), and Ox2-R4 (magenta) probes. **h**, DNA origami design. The distance between two adjacent docking sites is 18 nm. **i,** TDI-DNA-PAINT images show that 18 nm DNA origamis can be resolved after 5 min of imaging with 25

nM of Ox2-R4. Scale bars, 10 nm. **j**, Line profile showing a peak-to-peak distance of 18.6 nm between two detected spots in the origami structure shown in **g**. On average we detected a docking site distance of 18.9 ± 2.2 nm (SEM).

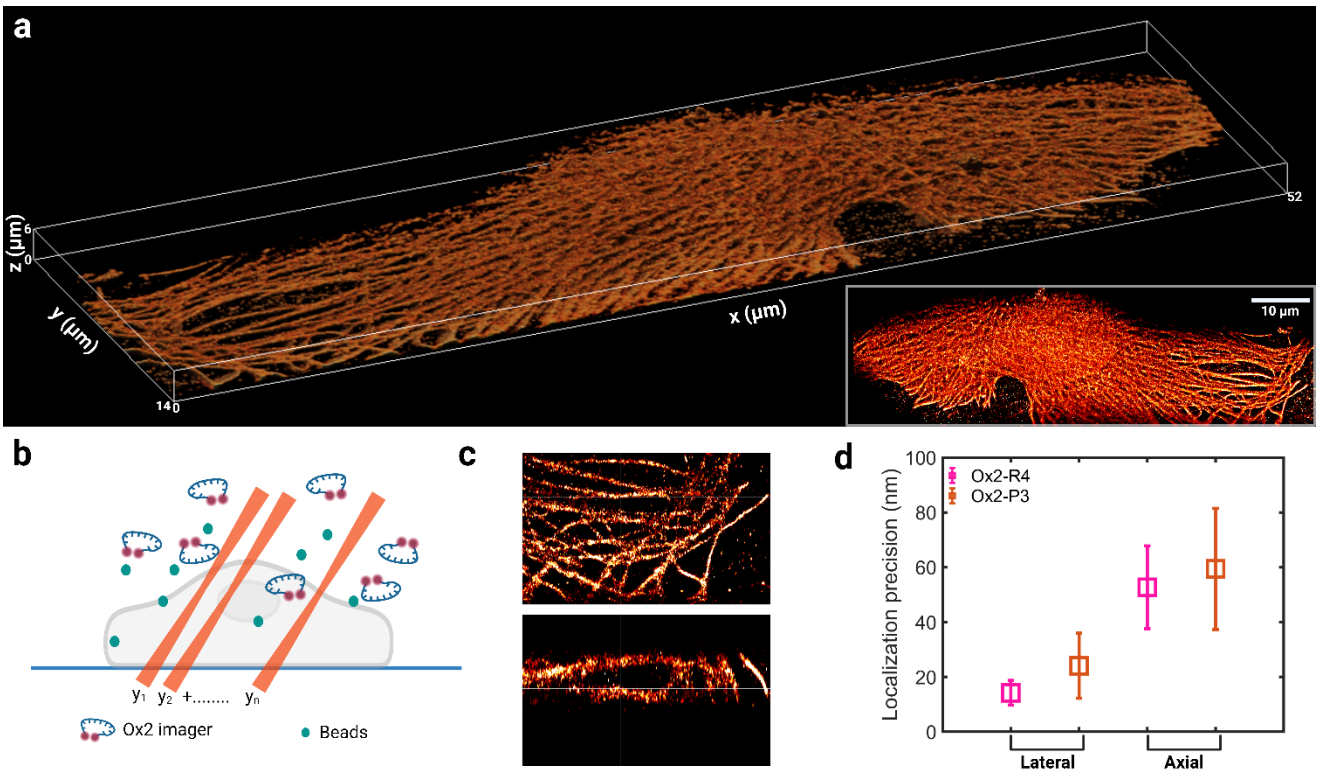

Fig. 2. Lattice light sheet (LLS) TDI-DNA-PAINT imaging. **a**, Whole-cell shadow projection volume rendering of a representative COS7 cell shows the microtubule network from TDI-DNA-PAINT imaging with Ox2-R4 probe. The bounding box is 52 µm × 14 µm × 6 µm. Inset illustrates a maximum *z* projection of the same cell after deskewing but before rotation to the actual coverslip coordinates. **b,** LLS TDI-DNA-PAINT workflow, a cell labeled with docking strands is fixed inside a glass-bottomed well and fluorescent beads are co-incubated for PSF calibration. Ox2-P3/R4 imager probes are used at a concentration of 2.5 nM. Using a light sheet of the dimensions 100 × 1.8 µm, the sample is imaged by acquiring a time series of 2,500 frames at one position along the skewed *y* axis before advancing to the next position with a step size of 500 nm. A total of 35 positions were imaged. **c,** Orthogonal views with *xy* (top) and *xz* (bottom) profiles of a representative ROI are shown. **d,** Localization precisions achieved from whole-cell LLS TDI-DNA-PAINT imaging for the cells shown in (a) and Extended data Fig. 2a. In case of Ox2-R4 (magenta), mean localization precisions of 24 nm and 59 nm were obtained along *x* and *z* respectively, whereas for Ox2-P3 (red) mean precisions were 14 nm and 53 nm, respectively, along lateral and axial directions.

Supplementary Information

Supplementary Information: Supplementary Fig. S1-S5 and description of LLS-TDI-DNA-PAINT imaging.